ChemPubSoc Europe

DOI: 10.1002/open.201900285

Open Access ChemistryOPEN Full Papers

Construction of Recycling Photocatalytic Gels for the Disinfection of Pathogens and Degradation of Organic Pollutants

Jinpeng Liu,[a] Nali Zhu,[b] Haiming Xu,[c] Jinwu Bai,[b] Chaofeng Shao,[a] Meiting Ju,[a] Qilin Yu,*[b] and Lu Liu*[a]

Bismuth oxybromide (BiOBr) nanosheets are exciting photocatalysts for microbial disinfection and organic dye degradation. However, it remains a great challenge to easily recycle these nanomaterials and improve their photocatalytic ability. Herein, we constructed a novel photocatalytic BiOBr@PAG gel containing BiOBr nanosheets and polyacrylamide gel (PAG), based on peroxydisulfate-induced polymerization reaction. The photocatalytic gel had equally distribution of BiOBr nanosheets on the surface, and could be easily recycled from water. More strikingly, the gel could also rapidly kill all tested pathogenic bacteria (i.e., *Escherichia coli*, *Pseudomonas aeruginosa*, and *Staphylococcus aureus*) under irradiation. Its disinfection activity is attributed to remarkable intracellular ROS production and oxidative cell damage. Furthermore, the gel had higher photocatalytic activity than BiOBr nanosheets alone during degradation of organic dyes. This study developed a novel strategy for preparation of easy-recycling and high-efficiency photocatalytic systems for practical application in environmental treatment and medicinal disinfection.

1. Introduction

With the development of emerging photocatalytic nanomaterials, photocatalysis is becoming a promising technique for application in a wide range of fields, such as environmental treatment, medicinal disinfection, CO_2 reduction and H_2 production.[1–3] Especially, photocatalytic degradation of organic pollutants (e.g., organic dyes), and microbial disinfection received great attention due to the increasing exposure of these hazardous factors to the environment and to the human bodies.[4–7] It is a hot topic to design novel, high-efficient convenient, and low-cost photocatalysts for removal of these factors from the environment.

Semiconductor nanomaterials, such as TiO_2 and ZnO, are the most studied photocatalysts.[8–10] However, these traditional semiconductor photocatalysts have wide band gap and hence could only absorb UV for catalysis, limiting their practical application.[10–13] In contrast, Bismuth oxybromide (BiOBr), an important V-VI-VII ternary semiconductor, process high stability and suitable band gaps for utilization of visible light for photocatalysis, hence broad perspectives in practice.[14,15] Up to now, BiOBr nanomaterials with different morphologies (mainly nanosheets and nanoflowers) has been developed as the catalysts for pollutant degradation and microbial disinfection.[14,16–18]

Although BiOBr nanomaterials, together with other photocatalysts, have received intensive studies in their synthesis and optimization of photocatalytic efficiency, it remains a great challenge to easily recycle the photocatalysts from the environment.[19,20] The difficulty of recycling these nanomaterials lead not only to high cost of the photocatalysts, but also to a significant and annoying pollution problem of these agents as consequent health risks.[21–23] Hence, it is urgent to construct easy-recycling photocatalytic systems for practical application.

In this study, based on peroxydisulfate-mediated polymerization reaction, we constructed a novel photocatalytic gel that was composed of BiOBr nanosheets and polyacrylamide gel (PAG), BiOBr@PAG (Figure 1). The photocatalytic gel not only could be easily recycled from the water, but also displayed enhanced photocatalytic properties as compared to BiOBr nanaosheets alone during microbial disinfection and organic dye degradation, realizing rapid removal of both pathogenic bacteria and organic pollutants from the water solution. This study developed a novel strategy for preparation of easy-recycling and high-efficiency photocatalytic systems for practical application.

[a] Dr. J. Liu, Dr. C. Shao, Prof. M. Ju, Prof. L. Liu
College of Environmental Science and Engineering, Nankai University, 38 Tongyan Rd., Tianjin 300350, China
E-mail: liul@nankai.edu.cn
[b] Dr. N. Zhu, J. Bai, Prof. Q. Yu
Key Laboratory of Molecular Microbiology and Technology, Nankai University, 94 Weijin Rd., Tianjin 300071, China
E-mail: yuqilin@mail.nankai.edu.cn
[c] Dr. H. Xu
Wuhan Textile University, Sch Environm Engn, Wuhan 430073, Hubei, China

Supporting information for this article is available on the WWW under https://doi.org/10.1002/open.201900285

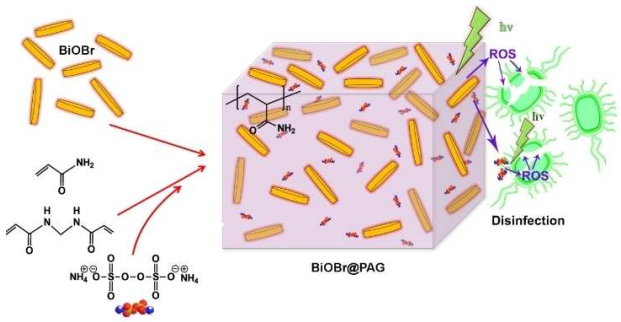

Figure 1. Schematic illustration of construction and disinfection mechanism of the BiOBr@PAG gel.

2. Results and Discussion

2.1. Properties of the BiOBr@PAG Photocatalytic Gel

The prepared BiOBr nanosheets were characterized by SEM and XRD. SEM revealed that the nanosheet had normal sheet-like morphology with a size ranging from 0.5 to 1 μm and an average thickness of about 20 nm (Figure S1A). XRD analysis showed that the nanosheets had regular XRD pattern which is consistent with standard spectrum of pure tetragonal phase BiOBr (Figure S1B).

The properties of the synthesized BiOBr@PAG photocatalytic gel were shown in Figure 2. SEM observation revealed that the BiOBr nanosheets were equally distributed, and most of the nanosheets were partially embedded in the gel and had clustering morphology on the gel surface (Figure 2A). EDS mapping further showed that the presence of expected elements, i.e., Bi, O, Br, N, and S, on the surface of the gel (Figure 2B). FT-IR spectrum demonstrated that the gel had representative groups, e.g., –CO–NH– (850 cm^{-1}, 1615 cm^{-1}, 3400 cm^{-1}) and $-CH_2-$ (2920 cm^{-1}) (Figure 2C). Thermogravimetric analysis further revealed that the weight of the dry gel gradually decreased ~70% during temperature increase from the room temperature to 420 °C, then suddenly decrease to 80% at 420 °C to 430 °C, and lastly decrease to <5% from 430 °C to 700 °C (Figure 2D). UV-vis-NIR diffuse reflection spectra (DRS) analysis further revealed that the BiOBr@PAG gel had much stronger light absorption across the entire examined spectral region, especially in the UV and NIR regions (Figure 2E), indicating a potential application under irradiation of the UV or NIR light. Moreover, the gel could be easily isolated from the water simply by precipitation or by filtration as compared to the BiOBr nanosheets (Figure 3A, 3B), indicating easy recycling of the gel during practical application.

In contrast, the BiOBr nanosheets had quite low disinfection ability, and only caused ~50% of decrease in cell viability (Figure 3A, 3B). This indicated that the gel had high-efficient disinfection activity against different pathogenic microbes under irradiation, which may facilitate its application in prevention and treatment of pathogen pollutions.

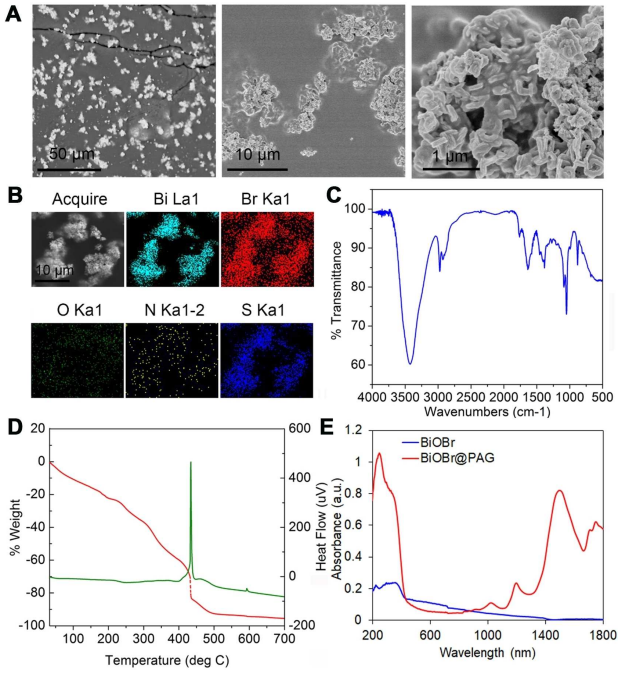

Figure 2. Characterization of the constructed BiOBr@PAG gel. (A) SEM images of the BiOBr@PAG gel. (B) EDS mapping images. (C) FT-IR spectrum. (D) Thermogravimetric analysis of the gel. (E) UV-vis-NIR DRS of BiOBr and BiOBr@PAG gel.

2.2. Disinfection by the BiOBr@PAG Photocatalytic Gel

Disinfection is always an important issue involved in environmental pollution treatment, food industry and medical practice.[24–26] Photocatalysis is a newly developing method of disinfection that has a great application potential.[27,28] We investigated the activity of the gel to kill several pathogenic bacteria, i.e., *Escherichia coli, Pseudomonas aeruginosa, and Staphylococcus aureus*. Under the dark condition, the BiOBr@PAG gel, similar to BiOBr nanosheets, had no obvious antibacterial effect (Figure S2). However, under the irradiation, both the gel and the BiOBr nanosheets displayed obvious killing ability to all of the tested bacterial strains, and the gel had significantly higher killing ability than the nanosheets alone (> 98% versus 35–50%) (Figure 4A–4C). For example, the gel showed time-dependent disinfection ability against *E. coli*, and led to almost 100% cell death after 30 min of irradiation (Figure 4A, 4B).

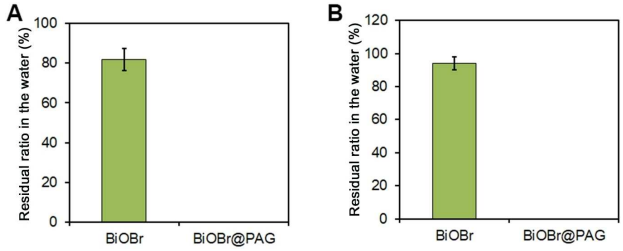

Figure 3. Residual ratio of BiOBr nanosheets and the BiOBr@PAG gel in the water after filtration using filter papers.

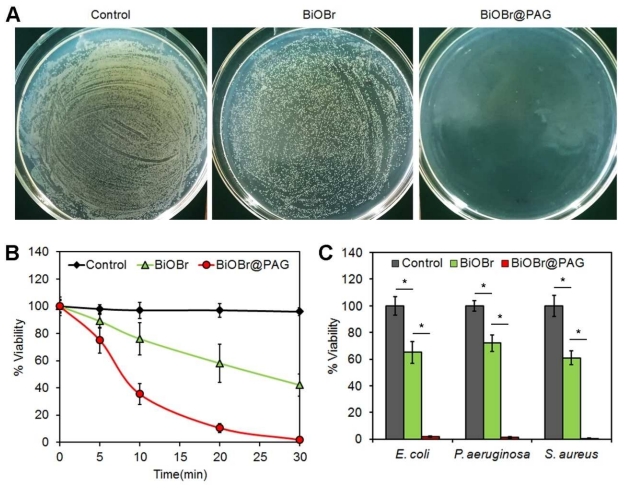

Figure 4. Disinfection of pathogenic bacteria by the BiOBr@PAG gel under irradiation. (A) Images of *E. coli* colonies after treatment of BiOBr (100 mg/L) or BiOBr@PAG (containing 100 mg/L BiOBr) with irradiation for 30 min. (B) Time-dependent disinfection activity of BiOBr or BiOBr@PAG against *E. coli*. (C) Disinfection activity of BiOBr or BiOBr@PAG against *E. coli*, *P. aeruginosa*, and *S. aureus* under irradiation. * indicates significant difference between the groups ($P < 0.05$).

ment of the BiOBr nanosheets, and its content decreased by ~30% after 30 min of irradiation (Figure 5A). In contrast, cell viability rapidly reduced by ~80% in 20 min under treatment of the BiOBr@PAG photocatalytic gel, and was almost thoroughly reduced 100% after 30 min (Figure 5B).

The cycling ability of disinfection of the BiOBr nanosheets and BiOBr@PAG gel was further detected. Although the nanosheets alone showed low photoinduced disinfection activity during the repeatedly photocatalytic processes, the BiOBr nanosheets had good cycling stability, with the photocatalytic activity only slightly impaired after 5 times of cycling (Figure 5C). Similarly, the photocatalytic activity of the gel was only slightly impaired by increase of the cycling times. Even after 5 times of cycling, the gel could also realize almost no impaired ability of disinfection (Figure 5D). Together, the BiOBr@PAG gel had much stronger and more disinfection activity than the BiOBr nanosheets alone, indicating an enhancement effect of gelation on photocatalytic ability of the nanosheets on the gel surface. Nevertheless, the photocatalytic activity of the gel was somewhat impaired after several times of recycling, indicating that the stability of the gel should be further enhanced by optimization of the construction components.

2.3. Rapid and Good-Cycling Disinfection by the BiOBr@PAG Photocatalytic Gel

The disinfection ability was further investigated by changing the irradiation time and the concentration of the gel. The disinfection activity was enhanced by the increase in BiOBr concentration. While the BiOBr even at 200 mg/L only caused <50% decrease of cell viability, the BiOBr@PAG gel at 100 mg/L or higher-concentration of BiOBr led to almost thorough 100% decrease (Figure 5A). Moreover, as the irradiation time increased, the cell viability gradually decreased under the treat-

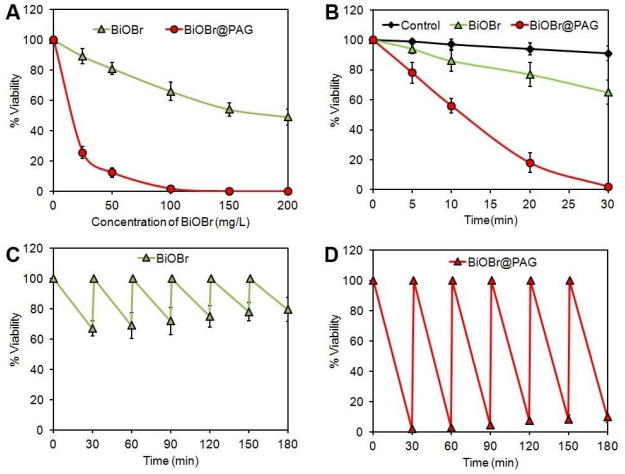

Figure 5. Concentration-dependent (A), time-dependent (B) and cycling ability (C, D) of disinfection caused by BiOBr nanosheets and BiOBr@PAG gel. (A) Concentration-dependent disinfection of *E. coli* cells. (B) Time-dependent disinfection. (C) Cycling of BiOBr nanosheet-catalyzed disinfection. (D) Cycling of BiOBr@PAG gel-catalyzed disinfection.

2.4. Severe Photoinduced Cell Death by the BiOBr@PAG Gel

Photocatalytic disinfection is commonly associated with plasma membrane (PM) damage of the microbial cells and consequent cell death.[29] Consistent with the results of cell viability assay, under the dark condition, both the gel and the BiOBr nanosheet did not cause obvious cell death (death rate <2%) (Figure 6A, 6 C). In contrast, under the irradiation condition, the gel led to

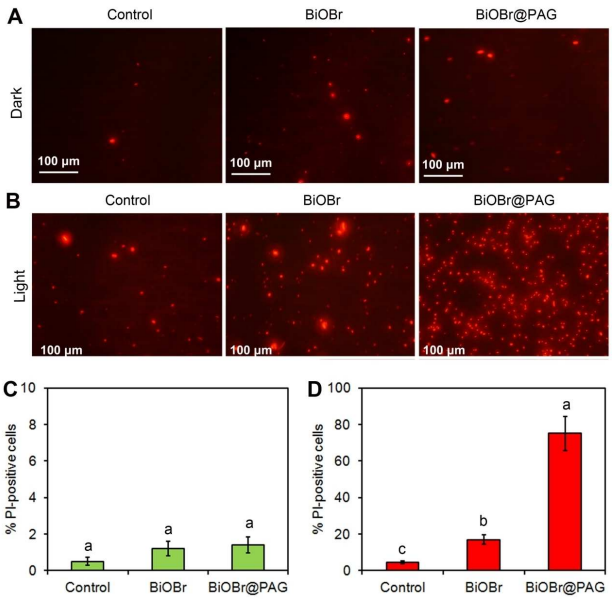

Figure 6. Cell death induced by the BiOBr nanosheets and BiOBr@PAG gel. (A, B) Fluorescence microscopy images of the cells under dark (A) and irradiation (B) conditions. (C, D) Quantification of PI-positive cells under dark (C) and irradiation (D) conditions. The same letters indicate no significant difference between the groups ($P < 0.05$).

severe cell death than the BiOBr nanosheet alone (70% versus 16%) (Figure 6B, 6D). This indicated that the gel may cause severe PM damage-related cell death under irradiation, and had much stronger photocatalytic disinfection activity than the BiOBr nanosheets.

2.5. Persulfate- and ROS-Dependent Photocatalytic Activity of the BiOBr@PAG Gel

It is interesting that the BiOBr@PAG gel showed much stronger photocatalytic disinfection activity than the BiOBr nanosheets. We wondered if the presence of PAG or APS contributed to the enhancement of photocatalytic activity. Indeed, PAG alone and APS alone had high and equivalent activity of disinfection (Figure 7A). Therefore, the presence of APS in the PAG gel played an important role in the gel-catalyzing process of dye degradation. Moreover, BiOBr nanosheets in combination of APS, similar to the BiOBr@PAG gel, displayed higher ability of disinfection than BiOBr, PAG or APS alone (Figure 7A). This indicated that other mechanisms, besides the presence of APS, might also contribute to irradiation-induced disinfection.

Considering that BiOBr is a photocatalyst, we proposed that photocatalysis may also be involved in the dye degradation. Since photocatalysis-induced disinfection depends on photo-induced production of ROS, followed by lipid oxidation and generation of MDA, we determined intracellular ROS and MDA levels under irradiation. As expected, the cells treated by the gel had much higher levels of ROS (0.77-fold higher) and MDA levels (2.2-fold higher) than the BiOBr-treated cells under irradiation (Figure 7B, 7 C). Similarly, PAG or APS could also induce increase in intracellular ROS levels, indicating that APS also contributed to ROS generation (Figure S3).

We then used the ROS scavengers (GSH and Vc) and the electron hole scavenger (KI) to investigate the role of ROS in disinfection.[30–32] While the addition of KI had no impact on dye degradation, addition of GSH and Vc led to remarkable increase of cell viability from $<2\%$ to $>60\%$ (Figure 7D), indicating that ROS scavengers, rather than electron hole scavenger, suppressed the gel-catalyzed disinfection. Taken together, both persulfate and ROS contributed to the photocatalytic activity of the BiOBr@PAG gel. Owing to the fact that the gel caused much higher ROS levels than BiOBr alone, we proposed that persulfate may lead to generation of intracellular ROS under irradiation of BiOBr, and both persulfate and BiOBr in synergy for enhancement of ROS production contributed to the higher disinfection ability of the gel than BiOBr nanosheets.

2.6. Rapid Degradation of Organic Dyes by the BiOBr@PAG Photocatalytic Gel

The photocatalytic ability of the prepared gel was further investigated during degradation of the organic dye brilliant green. As the irradiation time increased, the dye gradually degraded under the treatment of the BiOBr nanosheets, and its content decreased by ~23% after 10 min of irradiation (Figure 8A). Very interestingly, this dye rapidly reduced by ~70% in 1 min under treatment of the BiOBr@PAG photocatalytic gel, and was almost thoroughly degraded after 10 min (Figure 8A). Moreover, dye degradation was enhanced by the increase in BiOBr concentration. While the BiOBr even at 200 mg/L only caused $<25\%$ of dye degradation, the BiOBr@PAG gel at 50 mg/L or higher-concentration of BiOBr led to almost thorough dye degradation (Figure 8B).

The cycling ability of the BiOBr nanosheets and BiOBr@PAG gel was further detected. Similar to the results of disinfection, the photocatalytic activity of the gel was not impaired by

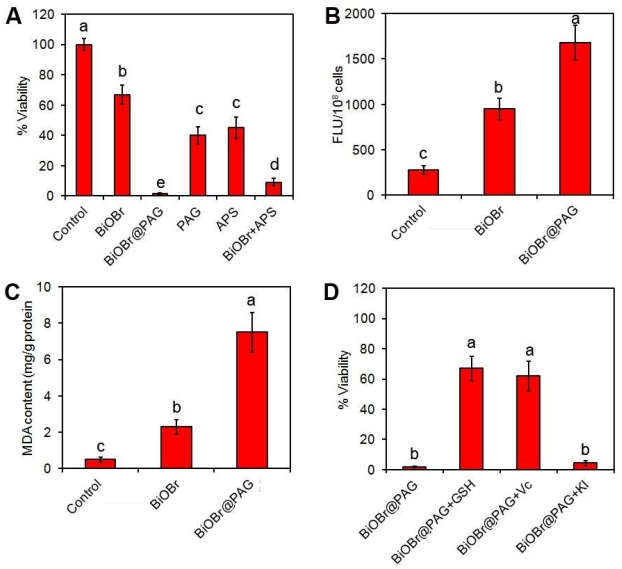

Figure 7. Effect of components of the BiOBr@PAG gel on viability (A), intracellular ROS levels (B), MDA levels (C), and effect of ROS scavengers on cell viability (D). The same letters indicate no significant difference between the groups ($P<0.05$).

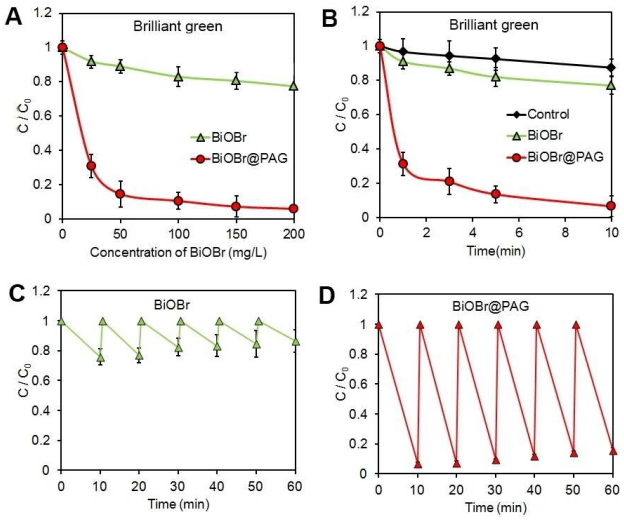

Figure 8. Photocatalytic degradation of brilliant green by BiOBr nanosheets and BiOBr@PAG gel. (A) Time-dependent degradation of brilliant green. (B) Concentration-dependent degradation. (C) Cycling of BiOBr nanosheet-catalyzed degradation. (D) Cycling of BiOBr@PAG gel-catalyzed degradation.

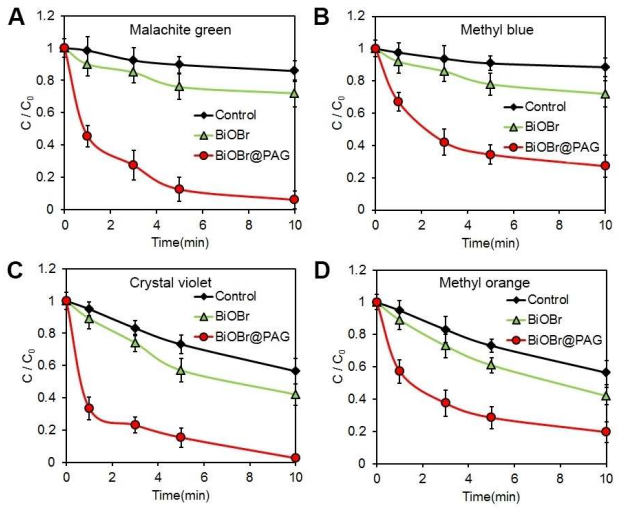

Figure 9. Photocatalytic degradation of malachite green (A), methyl blue (B), crystal violet (C) and methyl orange (D) by the BiOBr@PAG gel.

increase of the cycling times. Even after 5 times of cycling, the gel could also realize almost thorough dye degradation (Figure 8C, 8D). Moreover, both the gel and the nanosheets did not lead to decrease of dye concentration under dark condition, even after 10 min of adsorption time (Figure S4), excluding the role of adsorption in dye removal. In addition, the gel remained its normal volumes after the dye degradation (Figure S5). Taken together, these observations implied that the BiOBr@PAG gel had much stronger photocatalytic activity than the BiOBr nanosheets alone.

The degradation ability of the gel was further tested during degradation of other representative organic dyes, including malachite green, methyl blue, crystal violet, and methyl orange. Similarly, while the irradiation had only little impact on dye degradation, the BiOBr alone enhanced dye degradation from 20–50%. In contrast, the BiOBr@PAG gel caused high-efficient degradation of these dyes from 80% to >95% (Figure 9A–9D). Therefore, the prepared gel also had strong photocatalytic activity during degradation of a wide range of organic dyes.

3. Conclusions

In summary, this study developed a novel photocatalytic gel with BiOBr nanosheets equally distributed on the surfaces of the PAG gel. The gel displays high-efficient photocatalytic activity during disinfection of pathogenic bacteria and degradation of organic pollutants. The construction of this photocatalytic gel provides a novel strategy for development of easy-to-recycling and high-efficient photocatalytic system for a wide range of applications, such as photodynamic therapy of pathogen-related infections, environment pollution treatment and food preservation.

Experimental Section

Synthesis of BiOBr Nanosheets

The BiOBr nanosheets were synthesized by a hydrothermal method [16]. Briefly, 0.485 g of $Bi(NO_3)_3 \cdot 5H_2O$, 0.485 g of cetyltrimethylammonium bromide (CTAB), 20 mL of ethylene glycol and H_2O were added to a 50-mL Teflonlined stainless autoclave. The suspension was stirred magnetically for 30 min, and a white precipitate formed. Then the Teflonlined stainless autoclave was heated at 180 °C for 12 h. After cooling down to room temperature, the resulting precipitate was washed with distilled water and ethanol several times and dried at 60 °C for 6 h, obtaining the BiOBr nanosheets.

Preparation and Characterization of the BiOBr@PAG Photocatalytic Gel

To obtain the BiOBr@PAG photocatalytic gel, 10 mg of as-synthesized BiOBr nanosheets were suspended in 1 mL of the distilled water and sonicated for 10 min. Meanwhile, 1.0 g of acrylamide and 0.035 g of bisacrylamide were dissolved in 9 mL of distilled water and stirred for 10 min. The BiOBr nanosheet suspension was then added into the acrylamide/bisacrylamide solution. After addition of 100 μL of 10% ammonium peroxydisulfate (APS, W/V, prepared in distilled water) and 20 μL of N,N,N′,N′-tetramethylethylenediamine, the mixture was plated on a glass dish for gelation, obtaining the BiOBr@PAG photocatalytic gel. The gel was cut to cube-like pieces for further use. Calculation revealed that the obtained wet gel contained ~0.1% (W/W) of BiOBr and ~0.1% (W/W) of APS. To characterize the prepared gel, the pieces were dehydrated with 100% ethanol and dried at room-temperature, and then examined by field-emission scanning electron microscopy (FE-SEM, SU8000, Hitachi), Fourier transformed infrared spectra (FT-IR, Bio-Rad, FTS6000, USA), and a thermogravimetric analyzer (TG-DTA, Thermo plus EVO2, TG8121, Rigaku, Japan). The UV-vis-NIR DRS was taken on a Lambda 750 spectropho-tometer (Perking Elmer).

The recycling properties of the BiOBr nanosheets and the BiOBr@PAG gel were assessed in water by precipitation and by filtration methods. In precipitation method, the BiOBr nanosheets and the BiOBr@PAG gel were suspended in distilled water at a final BiOBr concentration of 100 mg/L and vortexed for 2 min. The suspensions were then stood for 1 min, and the supernatants were adsorbed for determination of the optical density at 630 nm (OD_{630}). In the filtration method, the vortexed suspensions were filtered by filtering papers, and OD_{630} of the filtrates were determined. The residual ratio of the materials was calculated by OD_{630} of the supernatants (or the filtrates) divided by the initial OD_{630}.

Disinfection Assay

To investigate the ability of the photocatalytic gel to kill the pathogenic bacteria, the clinically isolated strains, i.e., the *Escherichia coli* strain NE1, the *Pseudomonas aeruginosa* strain NP4, and the *Staphylococcus aureus* strain NS5, were used for disinfection assays. Briefly, the bacterial cells were overnight cultured in liquid Luria-Bertani (LB) medium, washed and suspended in PBS buffer (pH 7.4) to a final concentration of 5×10^6 cells/mL. BiOBr nanosheets or the BiOBr@PAG photocatalytic gel were then added into the cell suspension to a final BiOBr concentration of 100 mg/L. The mixtures were irradiated or not by the xenon light (100 W, OSRAM, Germany) for 10 min, sampled, and 10-fold gradient diluted for detection of colony formation unit (CFU) at LB plates.[33] The percent

of viability (% Viability) was calculated as the CFUs of the treatment divided by the CFUs of the control ×100%.

Cell Death Assay

To evaluate cell death caused by the BiOBr nanosheets or the BiOBr@PAG gel, the cells were treated by the nanosheets of the gel at dark condition or at the irradiation condition for 30 min. The cells were then harvested and stained by propidium iodide (PI, 5 mg/L) for 5 min, and then examined by a fluorescence microscope (Olympus, Japan). The percent of PI-positive cells were calculated.

Photocatalytic Cycling of Disinfection

To detect the cycling ability of the gel in disinfection, the gel (final BiOBr concentration of 100 mg/L) was added into the *E. coli* suspension (5×10^6 cells/mL), and then the mixture was irradiated for 30 min. The solution was then absorbed from the wells, and the *E. coli* suspension at the same concentration was added into the wells for further photocatalytic degradation. The degradation tests were repeated 5 times, and the percent of viability was calculated.

Investigation of Precursor Effect on Disinfection

The gel precursors, including BiOBr, PAG, APS, BiOBr plus APS, were used for investigation of precursor effect. Briefly, BiOBr (100 mg/L), PAG (100 g/L), APS (100 mg/L), and BiOBr (100 mg/L) plus APS (100 mg/L) were added into the *E. coli* suspension. The mixtures were then irradiated by the xenon light for 30 min for detection of viability.

ROS Assay

To determine ROS levels of the *E. coli* cells, the treated cells were stained by DCFH-DA (10 mg/L, Sigma, USA) for 40 min, and then washed twice by PBS buffer (pH 7.4). The fluorescent density (FLU, excitation wave 488 nm, emission wave 520 nm) was determined by a fluorescence microplate reader (PerkinElmer, USA). Cells were also counted using a hemocytometer. The relative fluorescence density of each sample was calculated as FLU divided by cell number to indicate intracellular ROS levels.

Malondialdehyde (MDA) Assays

To detected the intracellular MDA levels, the cells were broken by heating at 98 °C for 20 min, and then the supernatants were isolated by centrifugation at 12,000 rpm for 10 min. The MDA levels of the supernatants were determined by the MDA assay kit (Nanjing Jiancheng Bioengineering Institute, China), and total protein contents were analyzed by Commassie protein assay reagents.

Scavenging of ROS or Electron Holes

To examine the effect of scavengers of ROS or electron holes on gel-caused disinfection, the BiOBr nanosheets or BiOBr@PAG gel (final BiOBr concentration of 100 mg/L) were added into the *E. coli* suspension, and then the scavengers of reactive oxygen species (ROS), i.e., glutathione (GSH, 2 mM), vitamin C (Vc, 2 mM), or the scavenger of electron holes KI (20 mg/L) was added. The mixtures were then irradiated by the xenon light for 10 min, and the viability was detected.

Dye Degradation Assay

The photocatalytic activity of as-synthesized BiOBr nanosheets and BiOBr@PAG gel to degrade organic dyes, including brilliant green, malachite green, methyl blue, crystal violet, and methyl orange, were examined in water solvent. Firstly, the organic dyes were dissolved in distilled water to a final concentration of 20 mg/L. The BiOBr nanosheets or BiOBr@PAG gel were added into the solutions to a final BiOBr concentration of 100 mg/L or 0~200 mg/L. The mixtures were then irradiated by a xenon light (100 W, OSRAM, Germany) and samples at different time points in 0~10 min. The OD630 for brilliant green, malachite green and methyl blue, OD_{600} for crystal violet, and OD_{490} for methyl orange were detected by a UV/Vis spectrometer (SmartSpec Plus, BioRad, USA). The value C/C_0 was calculated as the optical density of the samples irradiated by the light for different time divided by the optical density of the samples at 0 min.

Acknowledgements

This work was supported by the National Natural Science Foundation of China (31870139, 31670146, 81873961, 81471923), the Tianjin Key Research and Development Plan (17YFNZNC00040, 19YFZCSN00450), the Tianjin Agricultural Science and Technology Achievement Conversion and Extension Project (201901130, 201901030), the Natural Science Foundation of Tianjin (17JCZDJC33300), and the Fundamental Research for the Central Universities.

Conflict of Interest

The authors declare no conflict of interest.

Keywords: photocatalysts · BiOBr nanosheet · polyacrylamide gel · disinfection · organic dye degradation

[1] W. Wang, M. O. Tadé, Z. Shao, *Chem. Soc. Rev.* **2015**, *44*, 5371–5408.
[2] N. Zhang, S. Liu, Y. J. Xu, *Nanoscale* **2012**, *4*, 2227–2238.
[3] I. Shown, H. C. Hsu, Y. C. Chang, C. H. Lin, P. K. Roy, A. Ganguly, K. H. Chen, *Nano Lett.* **2014**, *14*, 6097–6103.
[4] M. N. Chong, B. Jin, C. W. Chow, C. Saint, *Water Res.* **2010**, *44*, 2997–3027.
[5] J. C. Yu, W. Ho, J. Yu, H. Yip, P. K. Wong, J. Zhao, *Environ. Sci. Technol.* **2015**, *39*, 1175–1179.
[6] H. Cheng, B. Huang, P. Wang, Z. Wang, Z. Lou, J. Wang, X. Qin, X. Zhang, Y. Dai, *Chem. Commun.* **2011**, *47*, 7054–7056.
[7] P. Fernández-Ibáñez, M. I. Polo-López, S. Malato, S. Wadhwa, J. W. J. Hamilton, P. S. M. Dunlop, J. A. Byrne, *Chem. Eng. J.* **2015**, *261*, 36–44.
[8] J. Schneider, M. Matsuoka, M. Takeuchi, J. Zhang, Y. Horiuchi, M. Anpo, D. W. Bahnemann, *Chem. Rev.* **2014**, *114*, 9919–9986.
[9] K. M. Lee, C. W. Lai, K. S. Ngai, J. C. Juan, *Water Res.* **2016**, *88*, 428–448.
[10] Y. Qu, X. Duan, *Chem. Soc. Rev.* **2013**, *42*, 2568–2580.
[11] T. Giannakopoulou, I. Papailias, N. Todorova, N. Boukos, Y. Liu, J. Yu, C. Trapalis, *Chem. Eng. J.* **2017**, *310*, 571–580.
[12] E. M. Samsudin, S. B. A. Hamid, *Appl. Surf. Sci.* **2017**, *391*, 326–336.
[13] L. Saikia, D. Bhuyan, M. Saikia, B. Malakar, D. K. Dutta, P. Sengupta, *Appl. Catal. A* **2015**, *490*, 42–49.
[14] J. Li, Y. Yu, L. Zhang, *Nanoscale* **2014**, *6*, 8473–8488.
[15] J. Cao, B. Xu, H. Lin, B. Luo, S. Chen, *Chem. Eng. J.* **2012**, *185*, 91–99.
[16] H. Zhang, Y. Yang, Z. Zhou, Y. Zhao, L. Liu, *J. Phys. Chem. C* **2014**, *118*, 14662–14669.

[17] Y. Huang, H. Li, M. S. Balogun, W. Liu, Y. Tong, X. Lu, H. Ji, *ACS Appl. Mater. Interfaces* **2014**, *6*, 22920–22927.
[18] F. Yanfen, H. Yingping, Y. Jing, W. Pan, C. Genwei, *Environ. Sci. Technol.* **2011**, *45*, 1593–1600.
[19] P. Wan, J. Wang, X. Wang, H. Yu, J. Yu, M. Lei, Y. Wang, *Appl. Catal. B* **2013**, *132*, 452–459.
[20] C. F. Zhang, L. G. Qiu, F. Ke, Y. J. Zhu, Y. P. Yuan, G. S. Xu, X. Jiang, *J. Mater. Chem. A* **2013**, *1*, 14329–14334.
[21] Y. Fan, W. Ma, D. Han, S. Gan, X. Dong, L. Niu, *Adv. Mater.* **2015**, *27*, 3767–3773.
[22] F. Gottschalk, T. Sonderer, R. W. Scholz, B. Nowack, *Environ. Sci. Technol.* **2009**, *43*, 9216–9222.
[23] A. Menard, D. Drobne, A. Jemec, *Environ. Pollut.* **2011**, *159*, 677–684.
[24] N. Klamerth, S. Malato, A. Agüera, A. Fernández-Alba, G. Mailhot, *Environ. Sci. Technol.* **2012**, *46*, 2885–2892.
[25] H. Ölmez, U. Kretzschmar, *LWT-Food Sci. Technol.* **2009**, *42*, 686–693.
[26] K. Kümmerer, *Chemosphere* **2001**, *45*, 957–969.
[27] M. P. Reddy, A. Venugopal, M. Subrahmanyam, *Water Res.* **2007**, *41*, 379–386.
[28] S. Q. Guo, X. H. Zhu, H. J. Zhang, B. C. Gu, W. Chen, L. Liu, P. J. Alvarez, *Environ. Sci. Technol.* **2018**, *52*, 6872–6880.
[29] D. Xia, T. An, G. Li, W. Wang, H. Zhao, P. K. Wong, *Water Res.* **2016**, *99*, 149–161.
[30] S. H. Cherng, Q. Xia, L. R. Blankenship, J. P. Freeman, W. G. Wamer, P. C. Howard, P. P. Fu, *Chem. Res. Toxicol.* **2005**, *18*, 129–138.
[31] X. J. Guo, M. Zhen, H. Liu, L. Liu, *RSC Adv.* **2015**, *5*, 24777–24782.
[32] C. M. Hessler, M. Y. Wu, Z. Xue, H. Choi, Y. Seo, *Water Res.* **2012**, *46*, 4687–4696.
[33] L. S. Zhang, K. H. Wong, H. Y. Yip, C. Hu, J. C. Yu, C. Y. Chan, P. K. Wong, *Environ. Sci. Technol.* **2010**, *44*, 1392–1398.

Manuscript received: September 19, 2019